Mononuclear and Binuclear Tetrapyrido[2,3-a:3′,2′-c:2″,3″-h:3‴,2‴-j]phenazine (tphz) Ruthenium Complexes

André Gourdon* and Jean-Pierre Launay

Groupe Electronique Moléculaire, Centre d'Elaboration de Matériaux et d'Etudes Structurales, CNRS UP 8011, BP4347, 29 Rue Jeanne Marvig, 31055 Toulouse Cedex, France

Received March 19, 1998

The mono- and binuclear ruthenium complexes $[(tpy)Ru^{II}(tphz)](PF_6)_2 \cdot 3H_2O$ (**2**) and $[(tpy)Ru^{II}(tphz)Ru^{II}(tpy)](PF_6)_4 \cdot 3H_2O$ (**3**), where tphz (**1**) is the fully conjugated tetrapyrido[2,3-a:3′,2′-c:2″,3″-h:3‴,2‴-j]phenazine, have been prepared and characterized. The analysis of the intervalence band of the mixed-valence $[(tpy)Ru^{II}(tphz)Ru^{III}(tpy)]^{5+}$ showed that it belongs to the class II with an electron coupling parameter V_{ab} of 0.05 eV, much smaller than for the analogous class III 2,3,5,6-tetrakis(2-pyridyl)pyrazine (tpp) complex (V_{ab} = 0.4 eV). This discrepancy has been interpreted as a lack of adaptation of tphz to the chelation of the ruthenium atoms.

Introduction

Great attention in currently being paid to the study of electron and energy transfer in polynuclear transition metal complexes.[1] Bridging ligands based on 2,2′:6′,6″-terpyridine (tpy) allow the construction of linear rodlike polynuclear metal−tpy−spacer−tpy−metal complexes. The spacers described so far comprise polyynes,[2] polyphenylenes,[3] and porphyrins,[4] which can show, by rotation around a single bond, nonplanar conformations for which the electron transfer is significantly reduced. The shortest of these bis-tpy type ligands, the 2,3,5,6-tetrakis(2-pyridyl)-pyrazine (tpp) does not show this problem and has been widely studied. Some mono-, di-, and even trinuclear complexes of Fe, Ni, Co, Cu, Rh, Ru, Ir, and Os[5] have been prepared. The study of electron transfer in the mixed-valence dinuclear $[(tpy)-Ru-tpp-Ru(tpy)]^{5+}$ has shown[6] that strong electronic coupling was observed in this complex (V_{ab} = 0.4 eV). However, in these dinuclear tpp complexes, steric repulsion of the 3 and 3′ hydrogen atoms induces a twisting of the pyridine rings,[7] which reduces the planarity of the bridging ligand. As part of a study of electron transfer through fully conjugated polyaromatic molecules,[8] we were interested in the closely related fully planar tetrapyrido[2,3-a:3′,2′-c:2″,3″-h:3‴,2‴-j]phenazine (tphz, **1**) complexes (Figure 1).

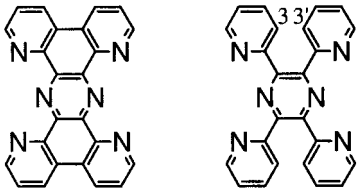

Figure 1.

Although **1** has been known for some time,[9] its coordination chemistry has not yet been studied, probably due to its lengthy (7 steps) and low yield (less than 5%) synthesis, starting from the expensive 4,7-phenanthroline. We have recently described a new 47% yield one-step synthetic route for this ligand,[10] which has opened the way to the preparation of its ruthenium inorganic complexes **2** and **3**, the first examples of fully conjugated ladders in the terpyridine series.

Experimental Section

Materials. 2,2′:6′,2″-terpyridine (tpy)[11] and $(tpy)RuCl_3$[12] were prepared according to the published methods. The bridging ligand tetrapyrido[2,3-a:3′,2′-c:2″,3″-h:3‴,2‴-j]phenazine (tphz, **1**) was obtained in moderate yield by condensation of 4,7-phenanthroline-5,6-dione[13] (phanquinone) in ammonium acetate at 180 °C according to ref 10a. All other solvents and reagents used were at least reagent grade quality and were used without further purification.

Methods and Instrumentation. UV−vis−near-IR spectra were taken on a Shimadzu UV-3100 spectrophotometer. FTIR spectra were obtained using a Perkin-Elmer 1725. Electrochemical measurements

* To whom correspondence should be addressed.

(1) Balzani, V.; Juris, A.; Venturi, M.; Campagna, S.; Serroni, S. *Chem. Rev.* **1996**, *96*, 759.
(2) (a) Grosshenny, V.; Harriman, A.; Ziessel, R. *Angew. Chem., Int. Ed. Engl.* **1995**, *34*, 1100. (b) Romero, F. M.; Ziessel, R. *Tetrahedron Lett.* **1994,** *35*, 9203. (c) Tsalis, D.; Tor, Y. *Chem. Commun.* **1996**, 1043.
(3) (a) Indelli, M. T.; Scandola, F.; Collin, J.-P.; Sauvage, J.-P.; Sour, A. *Inorg. Chem.* **1996**, *35*, 303. (b) Barigelletti, F.; Flamigni, L.; Balzani, V.; Collin, J.-P.; Sauvage, J.-P.; Sour, A.; Constable, E. C.; Cargill Thompson, A. M. W. *J. Am. Chem. Soc*. **1994**, *116*, 7692.
(4) Collin, J.-P.; Harriman, A.; Heitz, V.; Odobel, F.; Sauvage, J.-P *J. Am. Chem. Soc.* **1994**, *116*, 5679.
(5) (a) Ruminski, R.; Cambron, R. T. *Inorg. Chem.* **1990**, *29*, 1575. (b) Ruminski, R. R.; Kiplinger, J. L. *Inorg. Chem.* **1990**, *29*, 4581. (c) Thummel, R. P.; Chirayil, S. *Inorg. Chim. Acta* **1988**, *154*, 77. (d) Vogler, L. M.; Brewer, K. J. *Inorg. Chem.* **1996**, *35*, 818. (e) Vogler, L. M.; Scott, B.; Brewer, K. J. *Inorg. Chem.* **1993**, *32*, 898.
(6) Collin, J.-P.; Laine, P.; Launay, J.-P.; Sauvage, J.-P.; Sour, A. *J. Chem. Soc., Chem. Commun.* **1993**, 434.
(7) See the structure of $[(H_2O)_2Cu(tpp)Cu(H_2O)_2]^{4+}$: Graf, M.; Greaves, B.; Stoeckli-Evans, H. *Inorg. Chim. Acta* **1993**, *204*, 239.
(8) (a) Bolger, J.; Gourdon, A.; Ishow, E.; Launay, J.-P. *J. Chem. Soc., Chem. Commun.* **1995**, 1799. (b) Bolger, J.; Gourdon, A.; Ishow, E.; Launay, J.-P. *Inorg. Chem.* **1996**, *35*, 2937.
(9) (a) Case, F. H. *J. Heterocycl. Chem.* **1967**, *4*, 157. (b) Pfeiffer, F.; Case, F. H. *J. Org. Chem.* **1966**, *31*, 3383.
(10) (a) Gourdon, A. *Synth. Commun.* **1997**, *27*, 2893. (b) Bonhôte, P.; Wrighton, M. S. *Synlett* **1997**, 897.
(11) Jameson, D. L.; Guise, L. E. *Tetrahedron Lett*. **1991**, *32*, 1999.
(12) (a) Adcock, P. A.; Keene, F. R.; Smythe, R. S.; Snow, M. R. *Inorg. Chem.* **1984**, *23*, 2336. (b) Constable, E. C.; Cargill Thompson, A. M. W.; Tocher, D. A.; Daniels, M. A. M. *New J. Chem.* **1992**, *16*, 855.
(13) Druey, J.; Schmidt, P. *Helv. Chim. Acta* **1950,** *33*, 1080.

S0020-1669(98)00312-7 CCC: $15.00
Published on Web 09/16/1998

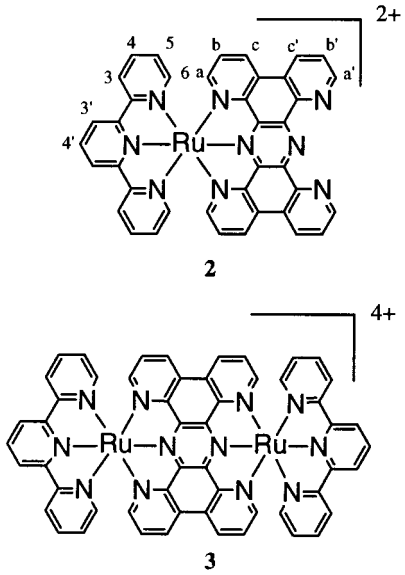

Figure 2.

were performed on an Electromat 2000 system. Cyclic voltammograms were obtained using a platinum working electrode, a platinum auxiliary electrode, and a saturated potassium chloride calomel reference electrode (Tacussel). At the end of each experiment, ferrocene was added and the couple Fc/Fc^+ potential was taken as an internal standard at 0.40 V. Linear and differential pulsed voltammetry were done using a platinum rotating disk electrode. The potentials were then automatically corrected for uncompensated cell resistance.[14] Mass spectra (CI and FAB) were recorded on a Nermag R10-R10 spectrometer. ^1H and $^1H-^1H$ NMR spectra were recorded on a Bruker DPX300 in acetonitrile-d_6. Chemical shifts were measured with reference to the solvent signal (1.96 ppm).

Syntheses. [(tpy)Ru(tphz)](PF$_6$)$_2$·3H$_2$O (2). A mixture of Ru(tpy)Cl$_3$ (50 mg, 0.113 mmol) and $AgBF_4$ (70 mg, 0.36 mmol) in acetone (50 mL) was refluxed for 2h. After filtration of AgCl, the acetone was evaporated and the residue was dissolved in DMF (10 mL). This solution was then added dropwise under argon to a suspension of **1** (50 mg, 0.13 mmol) in DMF (40 mL) at 120 °C. The solution was then stirred for 3 h at this temperature. After cooling and filtration, the solvent was evaporated under vacuum. The residue was then extracted with CH_3CN (100 mL). Addition of an aqueous solution (100 mL) of NH_4PF_6 (500 mg) and concentration under vacuum gave a brown precipitate, which was then washed with water and dried under vacuum. Chromatography on silica gel (acetonitrile, 1-butanol, water, saturated aqueous potassium nitrate (4:1:1:0.1 v/v) as eluent) gave an orange complex, which was obtained as a PF_6 salt by precipitation by NH_4PF_6 in warm water (80 mg, 66%). Anal. Calcd for $C_{39}H_{23}N_9F_{12}P_2Ru·3H_2O$: C, 44.08; H, 2.75; N; 11.86. Found: C, 43.86; H, 2.91; N, 11.84. FAB-MS (nitrobenzyl alcool matrix): 864 (M − PF_6); 719 (M − 2PF_6).^1H NMR (CD_3CN, 60 °C): atom labeling shown in Figure 2. Data include respectively chemical shift (ppm), attribution, number of protons, multiplicity, J (Hz), J' (Hz) (multiplicity abbreviations, s = singlet, d = doublet, dd = doublet of doublets, t = triplet, br = broad, not clearly resolved) 9.31, Hc′, 2H, d, 7.8; 9.20, Ha′, 2H, br; 9.16, Hc, 2H, d, 8.1; 8.98, H3′, 2H, d, 8.2; 8.70, H4′, 1H, t, 8.2; 8.63, H3, 2H, d, 7.7; 8.14, Hb′, 2H, dd, 7.8, 4.5; 8.02, Ha, 2H, d, 5.3; 7.94, H4, 2H, dd, 7.7, 6.0; 7.81, Hb, 2H, dd, 8.4, 5.3; 7.40, H6, 2H, br; 6.97, H5, 2H, dd, 6.0, 6.0.

[(tpy)Ru(tphz)Ru(tpy)](PF$_6$)$_4$·3 H$_2$O (3). The dinuclear complex was prepared in a similar way, by reaction of [Ru(tpy)(acetone)$_3$](BF$_4$)$_2$ (0.113 mmol) and **1** (20 mg, 0.05 mmol) in DMF (50 mL). After the mixture was stirred for 5 h at 120 °C under argon, cooling, filtration, and evaporation of the solvent gave a dark residue, which was chromatographied on silica gel (acetonitrile, 1-butanol, water, saturated aqueous potassium nitrate (4:1:1:0.2 v/v)). After elution of traces of $[Ru(tpy)_2]^{2+}$ and of orange mononuclear $[Ru(tpy)(tphz)]^{2+}$, the green fraction was collected. The solvent was then evaporated, and the product was dissolved in warm water; addition of NH_4PF_6 (500 mg) and cooling of the suspension gave a dark green powder, which was washed with warm water and dried under vacuum (24 mg, 28%). Anal. Calcd for $C_{54}H_{34}N_{12}F_{24}P_4Ru_2·3H_2O$: C, 38.45; H, 2.39; N, 9.96. Found: C, 38.15; H, 2.61; N, 9.83. FAB-MS (nitrobenzyl alcool matrix): 1489 (M − PF_6), 1344 (M −2PF_6); 1199 (M − 3PF_6); 1054 (M − 4PF_6).

Protonation of 2. The PF_6 salt [(tpy)Ru(tphz)](PF$_6$)$_2$ was dissolved in a minimum volume of acetone at room temperature. Addition of a 2-fold excess of NBu_4Br gave an orange precipitate of the bromide salt, which was washed with cold acetone and dried under vacuum. This salt is soluble in water. The solutions at various pHs were obtained by addition of aliquots of 1 mL solutions of the bromide salt (10^{-4} M) in water to aqueous solutions of hydrochlorhydric acid.

Calculations. The geometries of the binuclear complexes were obtained by molecular mechanics with the program Cerius2 (Biosym/Molecular Simulations) using the Universal Force Field.[15] Parametrization of the Ru−N distances was done using the 47 X-ray structures of the CSSR database[16] containing the Ru(tpy) fragment. The value Ru−N (pyridine) = 2.05 Å was used with an harmonic potential function and force constants k = 100 and 500 (kcal /mol) Å^2. The conformation used for calculations on the ligand tpp was extracted from the X-ray structure of $[(H_2O)_2Cu(tpp)Cu(H_2O)_2]^{4+}$.[7] Calculation of the electronic structure was then performed with the extended Hückel approximation using the program CACAO.[17]

Results and Discussion

Syntheses. The monomer complex **2** can be prepared by reaction of the bridging ligand **1** with the solvate precursor $[Ru(tpy)(acetone)_3]^{2+}$ in DMF, which was obtained by dechlorination of $[Ru(tpy)Cl_3]$ in acetone.[18] The dinuclear complex is similarly prepared by reaction of an excess of $[Ru(tpy)(acetone)_3]^{2+}$ with **1** in refluxing 1-BuOH. The products were purified by chromatography on silica gel. They were characterized by chemical analyses and FAB-MS with 3-nitrobenzyl alcohol as the matrix. In each case, the highest fragment ions only involved sequential loss of PF_6^- counterions.

^{1}H NMR. The proton NMR spectra of the complexes showed important broadening of some peaks at room temperature. This broadening could originate from (a) paramagnetism, (b) aggregation in solution, i.e., intermolecular movements or (c) intramolecular movements. A broadening by paramagnetism was not considered; addition of traces of reductors or oxidants did not improve at all the peaks widths.

Monometallic Complex 2. Aggregation in solution of ruthenium complexes bearing large polyaromatic ligands has been described recently.[5b] An increase of the NMR solution concentrations or a decrease of the temperature led to peak broadening and to upper-field shifts for the ligand protons. For the monometallic complex **2**, at low temperature (−20 °C), the peaks corresponding to the tphz protons Hc′, Ha′, Hc, and Hb′ and to the tpy peaks H5 and H6 are broad and unresolved (see Figure 3). With increasing temperature, most of these peaks

(14) Cassoux, P.; Dartiguepeyron, R.; Fabre, P.-L.; De Montauzon, D. *Electrochim. Acta* **1985**, *30*, 1485.

(15) (a) Rappé, A. K.; Colwell, K. S.; Casewit, C. J. *Inorg. Chem.* **1993**, *32*, 3438. (b) Rappé, A. K.; Casewit, C. J.; Colwell, K. S.; Goddard, W. A.; Skiff, W. M. *J. Am. Chem. Soc.* **1992**, *114*, 10024.

(16) Allen, F. H.; Davies, J. E.; Galloy, J. J.; Johnson, D.; Kennard, O.; Macrae, C. F.; Mitchell, E.; Smith, J. M.; Watson, D. G. *J. Chem.. Inf. Comput. Sci.* **1991**, *31*, 187.

(17) Mealli, C.; Proserpio, D. M. CACAO PC version 4.0, July 1994. *J. Chem. Educ.* **1990**, *67*, 399.

(18) See, for example: Beley, M.; Chodorowski, S.; Collin, J.-P.; Sauvage, J.-P.; Flamigni, L.; Barigelletti, F. *Inorg. Chem.* **1994**, *33*, 2543.

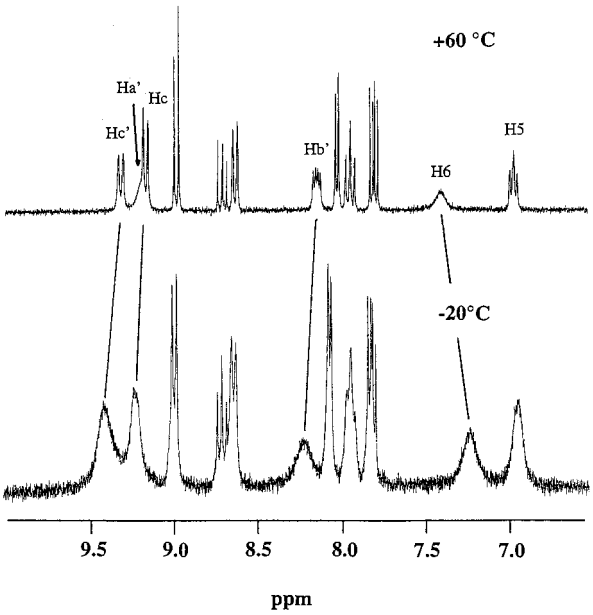

Figure 3. ^{1}H NMR spectra of **2** in CD_3CN at −20 and 60 °C.

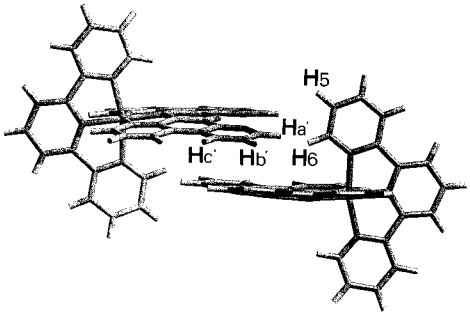

Figure 4. Model for the aggregation of **2**.

sharpen and get thinner so that at 60 °C, all peaks are well resolved except Ha′ and H6. Furthermore, the signals corresponding to the tphz protons move to higher fields, whereas the tpy protons move downfield. This behavior can be attributed to aggregation of the tphz parts as illustrated in Figure 4. These ^{1}H NMR spectra modifications are in agreement with those encountered in other complexes[5b] and in some host−guest organic complexes, catenanes, and rotaxanes. The 60 °C spectrum shows that the monometallic complex has the C_{2v} symmetry. In the absence of X-ray structures for these complexes, **2** and **3**, some insights into their geometry can be inferred from molecular modeling by comparison with published Ru−tpy distances and angles. A survey of the 47 X-ray structures containing the Ru(II)tpy fragment found in the literature shows that the average value for the $N_{lat}-N_{lat}$ (N_{lat} = lateral N) distance is 4.13 Å, for $Ru-N_{lat}$ is 2.06 Å, and for $Ru-N_{axial}$ is 1.95 Å, and for $N_{lat}-N_{axial}-N_{lat}$ the average angle is 104°. In free tphz or in tpy (in the cis−cis coplanar conformation), the $N_{lat}-N_{lat}$ distance is estimated to be 4.75 Å and the $N_{lat}-N_{axial}-N_{lat}$ angle around 120°. Therefore, the complexation of a ruthenium atom requires a pinching of the chelating site. The geometries of the complexes have been obtained by molecular mechanics using the Universal Force Field[14] (see experimental part). In the absence of reliable force-field parameters for the Ru−N bond, different geometries have been calculated depending upon the force constant of the Ru−N(tphz) bonds. As shown in Figure 5, the complexation of one of the terdentate sites induces a distortion of the tphz ligand, which keeps a nearly planar geometry but with an opening of

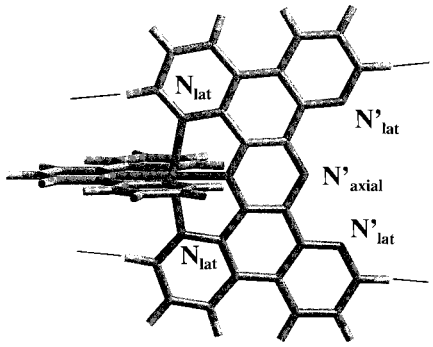

Figure 5. Distortion of the tphz ligand upon complexation in the monomer **2**.

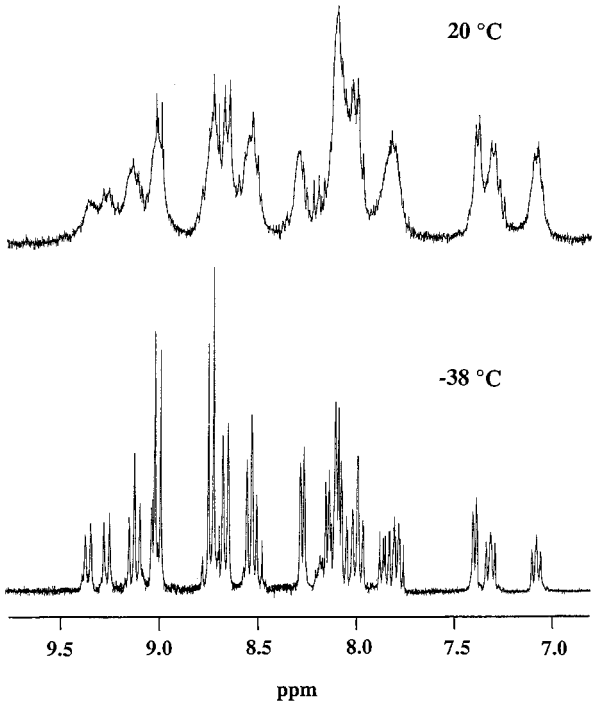

Figure 6. ^{1}H NMR spectra of **3** in CD_3CN at 20 and −38 °C.

the its free chelation site. Under these conditions, when the ruthenium atom is at tpy-type bonding geometry, with a $N_{lat}-N_{lat}$ distance of 4.13 Å, the $N'_{lat}-N'_{lat}$ distance increases to 5.13 Å, far too much for a terdentate chelation of a second ruthenium atom.

Dimetallic Complex 3. As shown in Figure 6, the ^{1}H NMR spectrum of **3** at room temperature shows also broad and poorly resolved signals. But contrary to the observed for **2**, this behavior does not improve with decreasing concentration or increasing temperature and cannot be attributed to an aggregation effect; indeed, in the case of this dimetallic complex, the short Ru−Ru distance and the important steric crowding precludes any efficient π-stacking of the tphz parts of two complexes. In contrast, the peak signals sharpen and get thinner with *decreasing* temperature giving at −38 °C a well-resolved pattern, which can be assigned to the superposition of the spectra of two species exchanging at a slow rate. From the monometallic species, the complexation of the second ruthenium atom can lead to two different geometries shown in Figure 7: (a) The Ru−N(tphz) distances are forced to that found in Ru−tpy fragments, which leads to a loss of planarity of tphz with a bowl-shaped geometry (Figure 7A) with a possible bowl-to-bowl inversion similar to that of corranulene[19] or (b) the ruthenium atoms are off-set from the molecule's 2-fold axis at

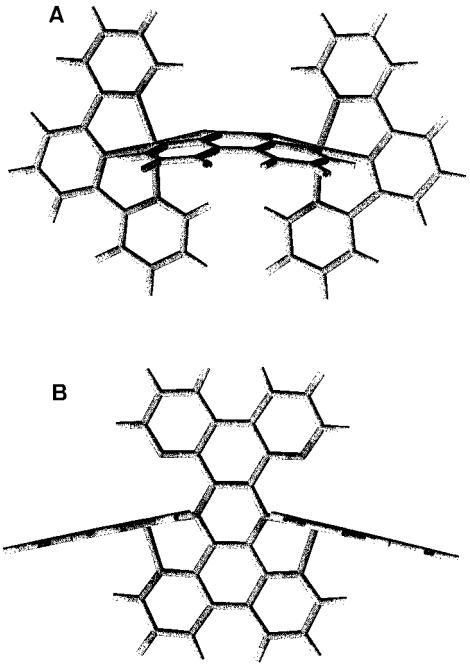

Figure 7. Molecular model of **3** in bowl (A) and planar (B, here cis isomer) conformations.

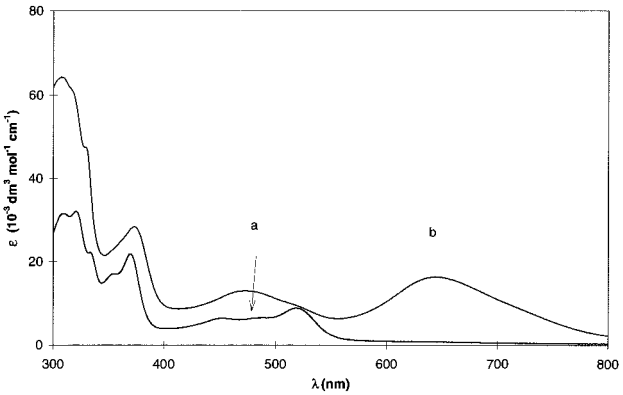

Figure 8. UV−visible absorption spectra of **2** (a) and **3** (b) in acetonitrile.

two more stable positions, at ca. 2.05 Å from the axial nitrogen atom N_{axial} and one of the two lateral nitrogen atoms N_{lat} (Figure 7B). In this bonding geometry, the complex **3** can be shown in the cis or in the trans isomers, depending on the location of the Ru(tpy) moieties. In this case, the intramolecular movement is a cis−trans inversion; at increasing temperatures, the exchange rate between the cis and the trans isomers quickens and, in the range of the NMR time scale, the peaks broaden and coalesce.

Despite the fact that it is not possible to fully assign with certainty the low-temperature COSY ^{1}H NMR spectra due to severe overlaps, a careful analysis shows that the observed tphz symmetry corresponds to hypothesis b (Figure 7B) with two isomeric species in a 1:1 ratio.

Absorption Spectra. The UV−visible parts of the absorption spectra of the mono- and dinuclear complexes **2** and **3** are shown in Figure 8 and collected in Table 1. Both tphz complexes show two main absorption bands in the visible part, attributed to the metal-to-ligand charge transfer (MLCT). The higher energy band at 450 nm for **2** and 472 nm for **3** can be attributed to a Ru-to-tpy transition by analogy with $[Ru(tpy)_2]^{2+}$ (475 nm). In

Table 1. Spectral Data[a]

species	absorption λ_{max}/nm (10^{-3} ϵ/dm^3 mol^{-1} cm^{-1})
1, tphz[b]	383 (9.4), 362 (8.8), 352 (7.7), 344 (8.2), 319 (21.7), 272 (33.3), 247 (24.8)
$[(tpy)Ru(tpp)]^{2+}$ [c]	474 (16), 310 (10.6), 274 (10.0), 224 (13.3)
2, $[(tpy)Ru(tphz)]^{2+}$	519 (8.9), 485 (7.0), 450 (6.8), 369 (18.9), 333(18.6), 320 (26.4), 308 (26.6), 274 (30.0)
$[Ru(tpy)_2]^{2+}$ [d]	475 (11.6), 307 (52.4), 270 (31.6)
$[(tpy)Ru(tpp)Ru(tpy)]^{4+}$ [b]	548 (36.0), 374 (33.0), 332 534.4), 300 (69.4), 274 (49.9)
3, $[(tpy)Ru(tpp)Ru(tpy)]^{4+}$	643 (16.3), 472 (12.4), 373 (30.1), 333 (52.7), 307 (71.3), 270 (77.0), 262 (78.9)

[a] PF_6 salts in acetonitrile. [b] In methanol/5% H_2O. [c] From ref 5c. [d] From ref 23b.

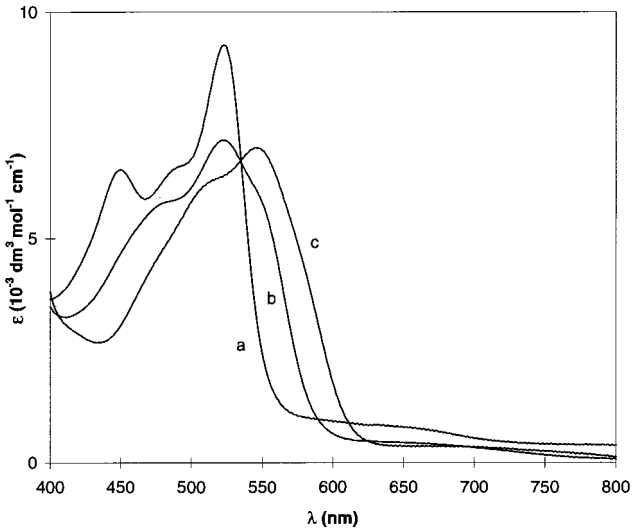

Figure 9. Visible part of the absorption spectrum of **2** at pH = 0.5 (a), 1.5 (b), and 7.0 (c).

2, the lower energy band at 519 nm is attributed to a Ru-to-tphz transition. This bathochromic shift reflects the strong π-acceptor character of tphz and its polyaromatic character, higher than that for tpy or tpp (the MLCT is at 474 nm in $[(tpy)Ru(tpp)]^{2+}$).[20] Extended Hückel calculation shows that in free tphz in the planar conformation, the HOMO−LUMO gap is 0.93 V (in the bowl conformation: 0.83 V), whereas it is 1.3 eV in tpp. As anticipated, this MLCT transition is shifted toward lower energies (643 nm) by stabilization of the LUMO upon coordination to a second metal center. This stabilization is significantly larger than that in $[(tpy)Ru(tpp)Ru(tpy)]^{4+}$, which shows an MLCT band at 548 nm. Once again the Ru-to-tpy transition at 472 nm is not affected by this red-shift, stressing the noninteracting character of the Ru(tpy) fragments as observed in other similar complexes.[21]

Protonation. As recently observed for the $[(ttpy)Ru(tpp)]^{2+}$ mononuclear complex,[22] the free tpy site of the mononuclear complex **2** can be protonated in acidic medium. Figure 9 shows the changes in the visible part of the absorption spectrum of **2** upon acidification in water. The most striking feature is a very significant bathochromic shift of the MLCT absorption maxi-

(19) Scott, L. T.; Hashemi, M. M.; Bratcher, M. S. *J. Am. Chem. Soc.* **1992**, *114*, 1920.

(20) Arana, C. R.; Abruna, H. D. *Inorg. Chem.* **1993**, *32*, 194 and references therein.

(21) This behavior has also been observed in similar complexes containing large aromatic ligands; see, for example: (a) Richter, M. M.; Brewer, K. J. *Inorg. Chem.* **1993**, *32*, 2827. (b) Downard, A. J.; Honey, G. E.; Phillips, L. F.; Steel, P. J. *Inorg. Chem.* **1991**, *30*, 2259.

(22) Barigelletti, F.; Flamigni, L.; Guardigli, M.; Sauvage, J.-P.; Collin, J.-P.; Sour, A. *J. Chem. Soc., Chem. Commun.* **1993**, 942.

Table 2. Half-Wave Potentials E (Volts) for the Oxidation E_{ox} and the Reduction E_{red} of the Ligand and the Complexes[a]

species	E_{ox1}	E_{ox2}	E_{red1}	E_{red2}	E_{red3}
$[Ru(tpy)]^{2+}$ [b]	1.32		−1.27	−1.52	
$[(tpy)Ru(tpp)]^{2+}$ [c]	1.50		−0.95	−1.40	−1.60
$[(tpy)Ru(tpp)Ru(tpy)]^{4+}$ [c]	1.40	1.71	−0.39	−0.86	−1.43 (2e$^-$), ir
1, tphz			−1.1		
2, $[(tpy)Ru(tphz)]^{2+}$	1.65		−0.61	−0.75	−1.26
3, $[(tpy)Ru(tphz)Ru(tpy)]^{4+}$	1.43	1.87	−0.24	−0.84	−1.5 (2e$^-$), ir

[a] Unless otherwise noted, the oxidation potentials are given vs SCE in CH_3CN and the reduction potentials are given vs SCE in DMF; the supporting electrolyte is 0.1 M NBu_4PF_6 at room temperature; the scan speed is 0.1 V s^{-1}. Except where indicated the processes were one-electron reversible processes. [b] Obtained vs SCE from ref 23b by addition of a Fc/Fc^+ (0.40 V) correction. [c] From ref 5c.

mum from 522 nm at pH 7 to 545 nm at pH 0.5. In these acidic solutions, all tphz free nitrogen atoms are protonated. As expected by analogy with similar complexes, this protonation has the same effect as a second coordination, with a lowering of the MLCT energy. The study of luminescence properties of **2** as a function of protonation is currently in progress.

Electrochemistry. a. Reduction. The electrochemical behaviors of the complexes have been studied in acetonitrile and in DMF (Table 2). In acetonitrile, the reductions are not well-behaved, probably due to the adsorption of the reduced species onto the surface of the platinum electrode, and show abrupt and sharp adsorption and desorption spikes. In DMF, this phenomenon disappears and the complexes display several reversible reduction processes. In this solvent, it was not always possible to observe the oxidative waves due to limitation by the solvent. Therefore, the oxidation potentials have been recorded in acetonitrile whereas the reduction potentials have been recorded in DMF. As a result of the poor solubility of the free tphz, it has not been possible to study its electrochemical behavior. The number of electrons involved in each redox process has been estimated by linear and pulsed differential voltammetry.

Cyclic voltammograms of the complexes **2** and **3** are consistent with metal-based reversible oxidations and several ligand-based reductions. By analogy with similar complexes, we assign the two first reductions at −0.61 and −0.75 V to successive reductions of tphz. The comparison with the mononuclear tpp complex, which shows two tpp reductions at −0.95 and −1.40 V emphasizes the stabilization of the LUMO in tphz (vide supra).

The one-electron reduction at −1.26 V is ascribed to the reduction of the tpy ligand, at the same potential as the first reduction of $[Ru(tpy)_2]^{2+}$, which shows that there is no influence of the first two electrons located on the tphz on the reduction potential of the tpy part.

For the dinuclear complex **3**, the two first reductions at −0.24 V and −0.84 V are similarly attributed to two reversible reductions of the bridging ligand **1**. The third reduction at ca. −1.5 V is clearly irreversible. It can be attributed to the reductions of the two tpy ligands, leading to a neutral species, which precipitates on the electrode.

b. Oxidation. The oxidation of the mononuclear complex **2** is reversible at 1.65 V, a potential more positive than that for $[Ru(tpy)_2]^{2+}$ (1.29 V) or $[(tpy)Ru(tpp)]^{2+}$ (1.50 V). Once again, the better π^* acceptor character of tphz stabilizes the ruthenium-based HOMO, rendering the oxidation of the metal more difficult.

The dinuclear complex **3** shows two reversible oxidation waves at 1.43 and 1.87 V, which can be attributed to the successive oxidations E_{ox1} and E_{ox2} of the two ruthenium centers

$$[(tpy)Ru^{II}(tphz)Ru^{II}(tpy)]^{2+} \overset{E_{ox1}}{\rightleftharpoons} [(tpy)Ru^{II}(tphz)Ru^{III}(tpy)]^{3+} \overset{E_{ox2}}{\rightleftharpoons} [(tpy)Ru^{III}(tphz)Ru^{III}(tpy)]^{4+}$$

The difference between the first and the second oxidation potentials for this dinuclear complex **3** is 440 mV, significantly larger than that for the analogous tpp complex (310 mV).[6] The comproportionation constant K_c calculated from this ΔE is 2.7×10^7 (1.7×10^5 for the tpp complex). Owing to this high value, no correction for disproportionation was necessary. The stability of the mixed-valent $Ru^{II}-tphz-Ru^{III}$ system calculated[24] by $\Delta G_{MV} = 0.5RT \ln(K_c/4)$ is 4.7 kcal, compared with ca. 2.5 kcal for tpp bridged complexes.

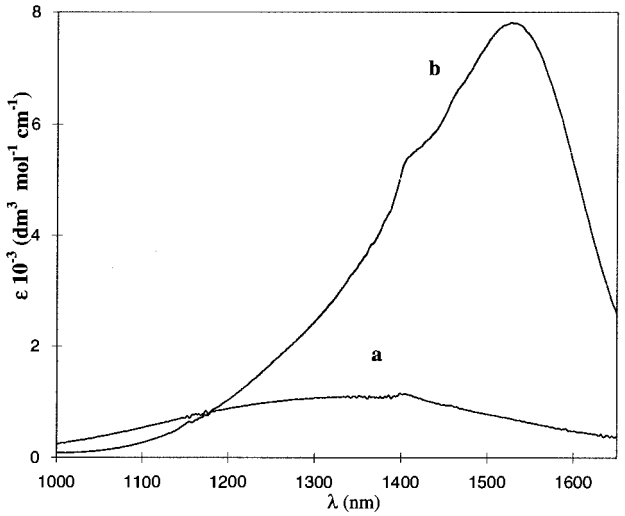

Figure 10. Intervalence bands of $[(tpy)Ru^{III}(tphz)Ru^{II}(tpy)]^{5+}$ (a) and $[(ttpy)Ru^{III}(tpp)Ru^{II}(ttpy)]^{5+}$ (b) complexes in acetonitrile. The bumps at 1180 and 1395 nm are uncompensated acetonitrile absorption bands.

Mixed-Valence Complex $[(tpy)Ru^{II}(tphz)Ru^{III}(tpy)]^{5+}$. Electrochemical oxidation of **3** at a potential between E_{ox1} and E_{ox2} yields the mixed valence species $[(tpy)Ru^{II}(tphz)Ru^{III}(tpy)]^{5+}$. This fairly unstable complex shows an intervalence transition at 1352 nm ($\epsilon = 1100$ M^{-1} cm^{-1}) with a bandwidth $\Delta\nu_{1/2} = 2214$ cm^{-1}. Figure 10 shows this intervalence band together with that of $[(ttpy)Ru(tpp)Ru(ttpy)]^{5+}$.[25] Although both complexes are structurally and electronically very similar, the differences between their intervalence bands[26] are striking. For the $[(ttpy)Ru(tpp)Ru(ttpy)]^{5+}$ complex, the intervalence band (b) is narrow ($\Delta\nu_{1/2} = 1145$ cm^{-1}), intense ($\epsilon = 7800$ M^{-1} cm^{-1}), and at low energy ($\lambda = 1530$ nm). Therefore, this compound seems to belong to class III, and the matrix element V_{ab}, taken as half the band energy, is 0.4 eV. In the case of $[(tpy)Ru^{II}(tphz)Ru^{III}(tpy)]^{5+}$, the intervalence band (a, Figure 10) is much broader, much weaker, and at higher energy so that this compound seems to belong to class II. In this hypothesis, the matrix element $V_{ab} = 0.050$ eV, calculated using the Hush's equation,[27] indicates a much smaller electronic coupling between the ruthenium atoms despite a higher com-

(23) (a) Young, R. C.; Nagle, J. K.; Meyer, T. J.; Whitten, D. G. *J. Am. Chem. Soc.* **1978**, *100*, 4773. (b) Constable, E. C.; Cargill Thompson, A. M. W. *J. Chem. Soc., Dalton Trans.* **1994**, 1409.
(24) Sutton, J. E.; Taube, H. *Inorg. Chem.* **1981**, *20*, 3125.
(25) Collin, J.-P.; Laine, P.; Sauvage, J.-P.; Sour, A. Private communication.
(26) Creutz, C. *Prog. Inorg. Chem.* **1983**, *30*, 1.

proportionation constant K_c and a smaller bridging ligand HOMO−LUMO gap. This result is puzzling but can be understood in the light of the low-temperature NMR results (vide supra).

The free energy of comproportionation is usually considered to depend on four factors:[26] an entropic factor, which is the same for both complexes; an electrostatic factor depending on the distance between the metal centers and is probably equal or even slightly larger for the tpp complex; the stabilization through electron delocalization, which is higher for the tpp complex; a synergistic factor ΔG_s which takes into account the stabilization of Ru(II) by Ru(III). (Note that this synergistic factor is an electronic effect and is related in some way to delocalization.) In the present case, we propose that a new effect, which is purely geometrical in origin, could contribute to ΔG_s; it is an "allosteric effect" by which a change in the coordination sphere of a ruthenium atom has consequences on the second coordination site. Modeling of the monometallic compound **2** has shown that pinching on one site widens the other site. In other respects, it is known that changing the oxidation state of a metal changes the metal−ligand bond lengths, with the oxidation process being accompanied by a shortening of the corresponding bonds.[26] Thus, in the bimetallic complex **3**, after oxidation of a first ruthenium atom (and thus contraction of its coordination sphere), the second site would be enlarged, i.e., brought to a geometry much less amenable to oxidation. This would shift the second wave to more positive potentials and thus increase the wave splitting and K_c. Such an effect would be purely geometrical and thus independent of the electronic delocalization process, which determines V_{ab}. Consequently, it is perfectly possible to have K_c and V_{ab} evolving in opposite directions from one compound to another.

As far as V_{ab} is concerned, it is puzzling that the more conjugated tphz ligand leads to a modest coupling when compared to tpp. Suspecting that the lack of adaptation of the coordination sites of tphz could play a role, we have performed a comparative minimization of the structures of [(ttpy)Ru(tpp)-Ru(ttpy)]$^{5+}$ and **3**, using the universal force field, with a force constant $k = 350$ (kcal /mol) Å^2 for Ru−N. It is found that the Ru−N axial bond is appreciably longer in **3** (2.036 Å in the cis isomer, Figure 7B) than in [(ttpy)Ru(tpp)Ru(ttpy)]$^{5+}$ (1.919 Å). Thus, in **3**, the ruthenium coordination to the bridging ligand is reminiscent of a coordination to a phenanthroline rather than a terpyridine and the difference in bond length is in agreement with crystallographic data on similar structures. Since the electronic interaction propagates essentially through the Ru−N_{axial} bond, this is an unfavorable situation in the case of **3**.

We have performed extended Hückel calculations[28] on both complexes and found indeed a modest *decrease* (−15%) in V_{ab} when going from [(ttpy)Ru(tpp)Ru(ttpy)]$^{5+}$ to **3**. In addition to the change in bond length, a second unfavorable factor occurs in **3**, namely a bad orientation of the relevant ruthenium orbital with respect to the axial N, as a consequence of the loss of symmetry. Thus, although we could not reproduce the magnitude of the change in V_{ab}, the theoretical calculations justify that contrary to intuition, the electronic interaction is smaller through tphz than through tpp.

Summary and Conclusion

The conjugated tetrapyrido[2,3-a:3′,2′-c:2″,3″-h:3‴,2‴-j]-phenazine (tphz) bridging ligand has been used to form the stable mono- and dinuclear complexes [(tpy)Ru^{II}(tphz)]$(PF_6)_2$ and [(tpy)Ru^{II}(tphz)Ru^{II}(tpy)]$(PF_6)_4$. The analysis of the intervalence band of the mixed-valence [(tpy)Ru^{III}(tphz)Ru^{II}(tpy)]$^{5+}$, obtained by electrochemical oxidation of the homovalent precursor, showed that it belongs to the class II with an electron coupling parameter of 0.05 eV, much smaller than that for the analogous class III [(ttpy)Ru(tpp)Ru(ttpy)]$^{5+}$ complex ($V_{ab} = 0.4$ eV). This discrepancy has been interpreted as a lack of adaptation of the rigid tphz to the chelation of the ruthenium atoms.

Acknowledgment. CIBA-GEIGY is gratefully acknowledged for the gift of phanquinone used for the synthesis of tphz. V. Duprez is thanked for assistance, S. Richelme and C. Claparols (Service Commun de Spectrometrie de Masse, Universite P. Sabatier, Toulouse) for mass spectroscopy experiments, and G. Pelletier (LCC, Toulouse) for low-temperature NMR studies. We thank also the CNRS for financial support of this work. Finally, J. P. Collin, P. Laine, J. P. Sauvage, and A. Sour are gratefully acknowledged for allowing us to use unpublished results on the [(ttpy)Ru(tpp)Ru(ttpy)]$^{5+}$ complex.

Supporting Information Available: Tables of atomic coordinates used for extended Huckel calculations (6 pages). Ordering information is given on any current masthead page.

IC980312R

(27) Hush, N. S. *Coord. Chem. Rev.* **1985**, *64*, 135.

(28) For other examples of V_{ab} determinations using extended Hückel calculations, see: (a) Patoux, C.; Launay, J.-P.; Beley, M.; Chodorowski-Kimmes, S.; Collin, J.-P.; James, S.; Sauvage, J.-P. *J. Am. Chem. Soc.* **1998**, *120*, 3717. (b) Larsson, S. *J. Am. Chem. Soc.* **1981**, *103*, 4034. (c) Larsson, S. *J. Chem. Soc., Faraday Trans. 2* **1983**, *79*, 1375. (d) Larsson, S. *J. Phys. Chem.* **1984**, *88*, 1321. (e) Siddarth, P.; Marcus, R. A. *J. Phys. Chem.* **1990**, *94*, 2985.